

Introduction

- There is a wide class of **space and astrophysical plasmas** where non-ideal MHD effects are important (such as 2-fluid), high frequency or short scales.
- Extended MHD (XMHD)** is formally 1-fluid model endowed with 2-fluid effects: **electron inertia** and **Hall drift** described by **IMHD** and **HMHD** limits respectively.
- These mutually exclusive effects were **unified in a Hamiltonian model** [5].
- Advantages of Hamiltonian methods include:
 - Systematic means for constructing equilibria, e.g. Beltrami flows.
 - Clear derivation of reduced models avoiding introduction of spurious dissipation.
 - Extraction of invariants such as helicity that plays a major role in this study.
 - Understanding of how collisionless reconnection operates by taking advantage of the underlying Hamiltonian structure
 - Natural means of arriving at weak turbulence theories.
 - Useful in constructing numerical integrators that automatically conserve invariants.
- Geometrical and topological properties of generalized helicities are investigated [7].
- Unusual connection between XMHD and Chern-Simons theory (TQFT) explored [7].
- Energy and helicity cascades are studied in **3D XMHD turbulence** [1].
- Study addresses recent interest in **sub-electron scales** that have become observable.

The Model: extended magnetohydrodynamics (XMHD)

Adopting XMHD ordering with electron inertia effects up to first order in electron mass.

$$\rho \left(\frac{\partial \mathbf{V}}{\partial t} + \mathbf{V} \cdot \nabla \mathbf{V} \right) = -\nabla p + \mathbf{J} \times \mathbf{B} - d_e^2 \mathbf{J} \cdot \nabla \frac{\mathbf{J}}{\rho} \quad (1)$$

The generalized Ohm's law (assuming $T_i < T_e$ we ignore ion pressure $p_e \gg p_i m_e/m_i$):

$$\mathbf{E} + \mathbf{V} \times \mathbf{B} = d_i \underbrace{\frac{\mathbf{J} \times \mathbf{B} - \nabla p_e}{\rho}}_{\text{Hall term}} + d_e^2 \left[\frac{\partial \mathbf{J}}{\partial t} + \mathbf{V} \cdot \nabla \frac{\mathbf{J}}{\rho} + \frac{\mathbf{J}}{\rho} \cdot \nabla \mathbf{V} \right] - d_i d_e^2 \frac{\mathbf{J}}{\rho} \cdot \nabla \frac{\mathbf{J}}{\rho} \quad (2)$$

Here $d_{i,e} = c/(\omega_{pe,i} \ell)$ are ion and electron skin depths normalized to scale length ℓ and $\omega_{pe,i}$ are the respective plasma frequencies. Normalized Alfvén units used.

$$\text{Total Energy: } H = \int_D d^3x \left[\frac{\rho V^2}{2} + \rho U(\rho) + \frac{B^2}{2} + d_e^2 \frac{|\nabla \times \mathbf{B}|^2}{2\rho} \right]. \quad (3)$$

Common Hamiltonian structure of XMHD brackets

Hall MHD is equipped with a noncanonical bracket [2] (barotropic equation of state):

$$\{F, G\}^{HMHD} = \{F, G\}^{MHD} + d_i \int_D d^3x \frac{\mathbf{B}}{\rho} \cdot \left[\left(\nabla \times \frac{\delta F}{\delta \mathbf{B}} \right) \times \left(\nabla \times \frac{\delta G}{\delta \mathbf{B}} \right) \right] \quad (4)$$

$$\text{Nontrivial coordinate change [5]} \quad \{F, G\}^{XMHD} \equiv \{F, G\}^{HMHD} [d_i - 2\kappa_{\pm}; \mathbf{B}_{\pm}], \quad (5)$$

where $\kappa^2 - d_i \kappa - d_e^2 = 0$; $\mathbf{V}_{\pm} = \mathbf{V} - \kappa_{\mp} \nabla \times \mathbf{B}/\rho$ and $\mathbf{B}_{\pm} = \mathbf{B}^* + \kappa_{\pm} \nabla \times \mathbf{V}$
 Because the bracket is noncanonical it exhibits Casimirs C such that $\forall F: \{F, C\} = 0$.

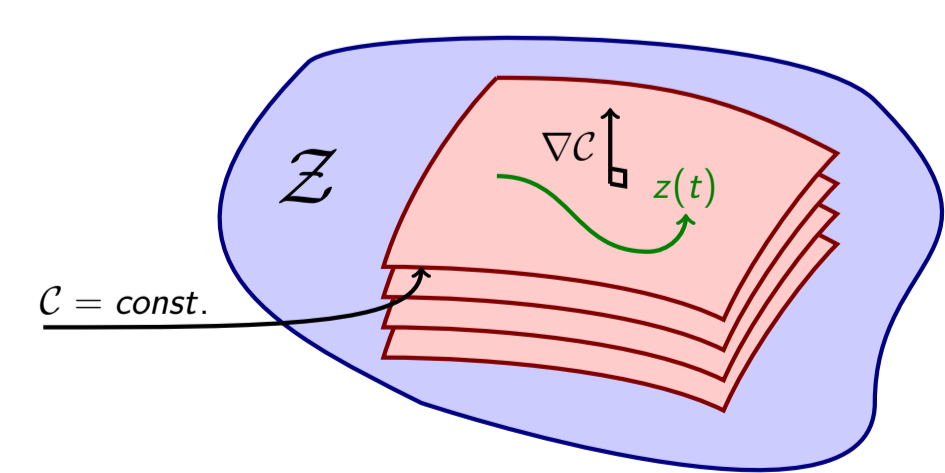


Figure: Foliation of phase space Z by Casimirs C in finite dimensions. Observe how dynamical system evolves ($z = z(t)$) on individual Casimir leaves. But field theories like XMHD are uncountably infinite dimensional!

$$C_- = \int_D d^3x \mathbf{A} \cdot \mathbf{B}, \quad (6)$$

Magnetic Helicity

$$C_+ = \int_D d^3x (\mathbf{A} + d_i \mathbf{V}) \cdot (\mathbf{B} + d_i \nabla \times \mathbf{V}),$$

Canonical Helicity

Under (5) one obtains more general XMHD Casimirs (Kinematical Constants of Motion):

$$\mathbf{B}^* = \mathbf{B} + d_e^2 \nabla \times \left[\frac{\nabla \times \mathbf{B}}{\rho} \right], \quad C_{\pm}^{XMHD} = \int_D d^3x (\mathbf{A}^* + \kappa_{\pm} \mathbf{V}) \cdot (\mathbf{B}^* + \kappa_{\pm} \nabla \times \mathbf{V}) \quad (7)$$

Generalized helicity conservation through the geometric lens

Let A_{\pm} be a 1-form associated with the components of general. vector potential \mathcal{A}_{\pm} and generating the 2-form $B_{\pm} = dA_{\pm}$ and the 3-form $C_{\pm} = A_{\pm} \wedge dA_{\pm}$, XMHD [7] has

$$\text{Lie-dragging } \frac{\partial A_{\pm}}{\partial t} + \underbrace{\mathcal{L}_{\mathbf{V}_{\pm}} A_{\pm}}_{\text{Lie Derivative}} = d\psi_{\pm}; \quad d^2 = 0 \Rightarrow \frac{\partial B_{\pm}}{\partial t} + \mathcal{L}_{\mathbf{V}_{\pm}} B_{\pm} = 0 \quad (8)$$

In coordinates (8) means $\frac{\partial B_{\pm}}{\partial t} = \nabla \times (\mathbf{V}_{\pm} \times \mathbf{B}_{\pm})$ leading to **frozen-in condition**

$$\frac{d}{dt} \int_{S_{\pm}(t)} \mathbf{B}_{\pm} \cdot d\mathbf{S} \Big|_{t=t_0} = \frac{d}{dt} \int_{S_{\pm}(t)} B_{\pm}(t) \Big|_{t=t_0} = \int_{S_{\pm}(t_0)} \frac{\partial B_{\pm}}{\partial t} + \mathcal{L}_{\mathbf{V}_{\pm}} B_{\pm} \Big|_{t=t_0} = 0, \quad (9)$$

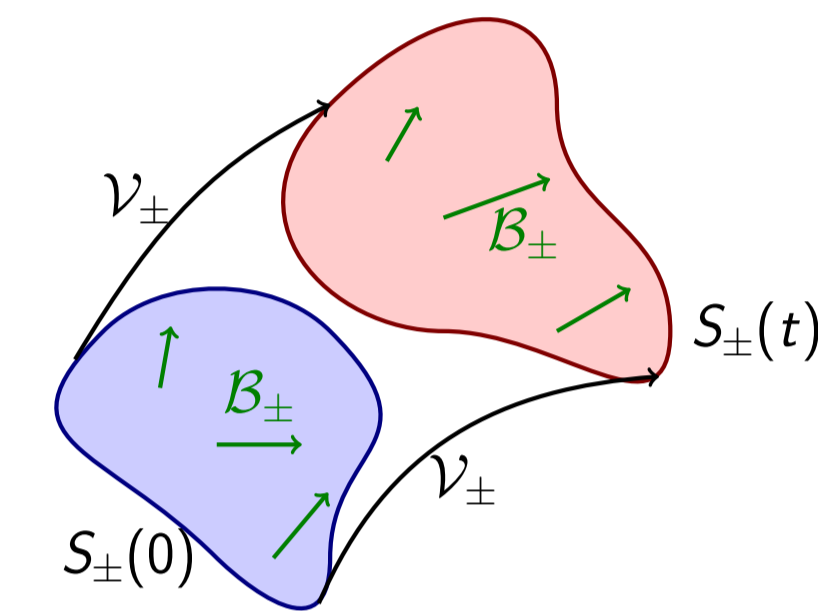


Figure: Schematics of two generalized frozen-flux constraints $\mathbf{B}_{\pm} \cdot d\mathbf{S}_{\pm} = \mathbf{B}_{\pm}^0 \cdot d\mathbf{S}_{\pm}^0$, where $d\mathbf{S}_{\pm}$ denote the corresponding area elements. It is possible to view the same statement as Lie dragging.

for 3-form dual to helicity density we have

$$\frac{\partial C_{\pm}}{\partial t} + \mathcal{L}_{\mathbf{V}_{\pm}} C_{\pm} = d\psi_{\pm} \wedge dA_{\pm} = d(\psi_{\pm} dA_{\pm}),$$

$$\frac{d}{dt} \int_{V_{\pm}(t)} C_{\pm} = \int_{\partial V_{\pm}(t)} \psi_{\pm} dA_{\pm} = 0, \quad (10)$$

Thus, **Conservation of generalized helicities** (Casimir invariants) can be encapsulated in geometric terms as the Lie-dragging of 3-forms.

Topological aspects of XMHD

Flux $\psi := \int_{S_{\pm}(t)} \mathbf{B}_{\pm} \cdot d\mathbf{S}$ of a filament with an axis of a given Twist and Writhe.

$$\text{Helicity in a filament decomposition } C = \sum_i \psi_i^2 (TW_i + Wr_i) + \sum_{ij} \psi_i \psi_j Lk_{ij}, \quad (11)$$

self-linking Gauss-linking

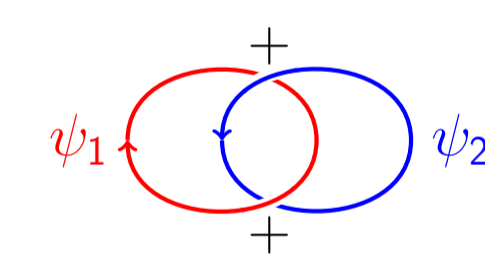


Figure: Helicity of linked flux tubes. $C = \int d^3x \mathcal{A} \cdot \mathcal{B} = \psi_1 \psi_2 + \psi_2 \psi_1$.

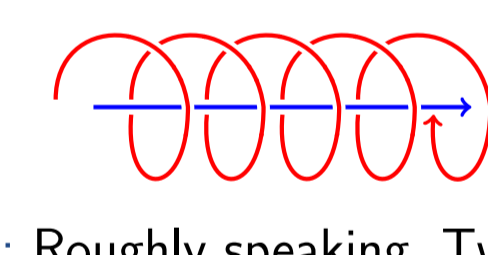


Figure: Roughly speaking, Twist measures number of windings of an outer field line around the axis.

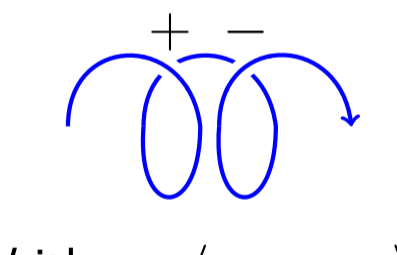


Figure: Writhe = $(\nu_+ - \nu_-)$, measures self-crossing number of the axis averaged over solid angle.

- Problem: Linking numbers do not distinguish between distinct topologies.
- Solution: Knot polynomials.

$$S_{CS} = \int_{\mathcal{M}} \left(P \wedge dP + \frac{2}{3} P \wedge P \wedge P \right),$$

helicity-like non-Abelian term

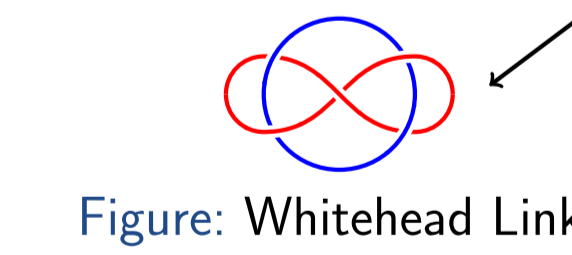


Figure: Whitehead Link

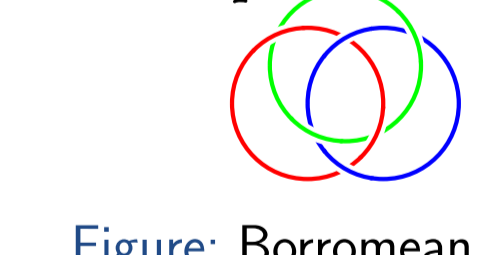
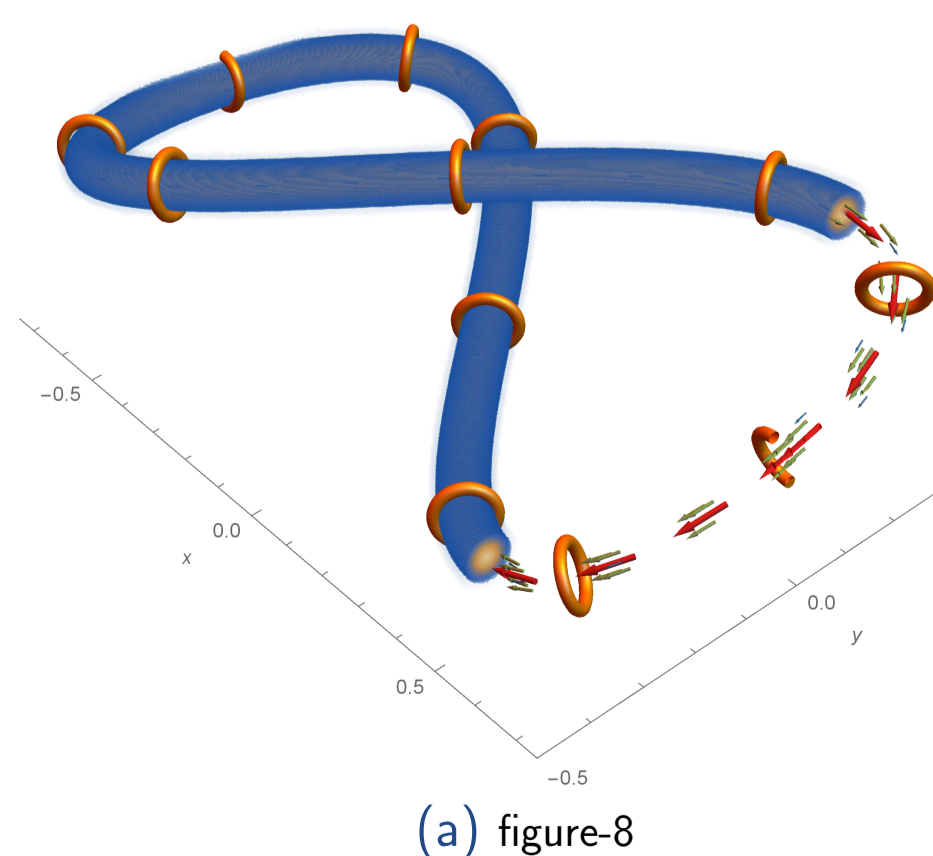
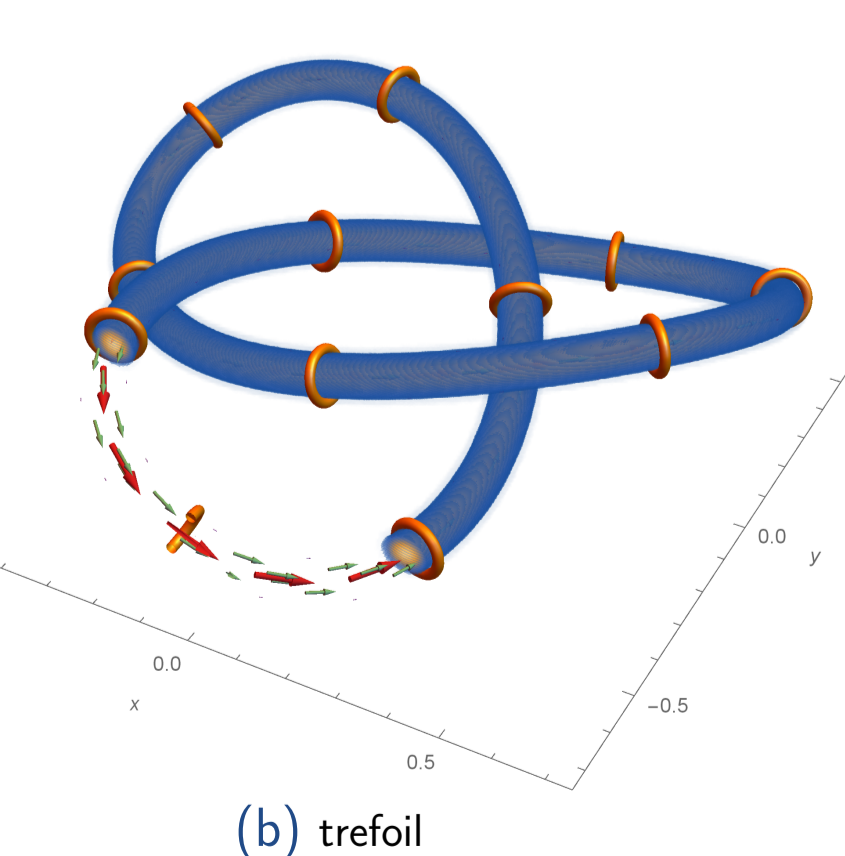


Figure: Borromean Links

- In fluids [6] $e^{\int d^3x v \cdot \nabla \times v}$ satisfies skein relations of Jones polynomial (some assump.).
- We propose [7] the use of Jones polynomials in XMHD (2 of them for each helicity).



(a) figure-8



(b) trefoil

Figure: Numerically constructed filament-like tube in the form of figure-8 and trefoil. Magnetic field around the axis has a Gaussian profile and is parallel to the axis. Orange rings show current density stream lines at chosen locations. (a) The axis has $Wr \approx .717$ but the tube is framed to have $Tw = 0$, i.e. field vectors are parallel to the axis (displayed by arrows). (b) The axis has $Wr \approx 3.22$ but the tube is framed to have $Tw = 0$. In both cases helicity is numerically confirmed to be due to Writhe linking. This requires finding associated vector potential, e.g. by solving Poisson's equation with the appropriate B.C.

3D Turbulence in incompressible extended MHD

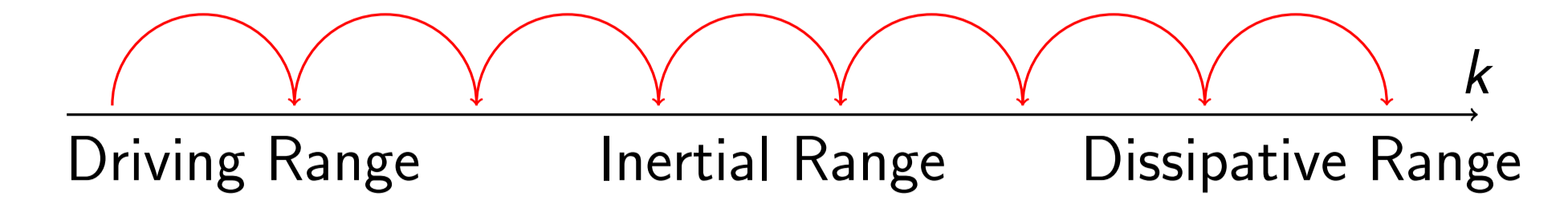


Figure: Schematics of a standard Richardson-Kolmogorov direct cascade. Energy is injected in low k , for e.g. via large scale stirring, cascades (flows) through the inertial range and dissipates at small scales (large k). Upon reversal of the arrows along with the driving and dissipative ranges, the mechanism of the inverse cascade is obtained.

Symmetric two-point correlations (taken at \mathbf{x}' and \mathbf{x}) of generalized helicities satisfy

$$0 = \frac{\partial}{\partial t} \frac{1}{2} \langle \mathcal{A}'_{\pm} \cdot \mathcal{B}_{\pm} + \mathcal{A}_{\pm} \cdot \mathcal{B}'_{\pm} \rangle = - \underbrace{\langle \delta(\mathbf{V}_{\pm} \times \mathbf{B}_{\pm}) \cdot \delta \mathbf{B}_{\pm} \rangle}_{\text{helicity flux rate}} + D \quad (12)$$

- More symmetry than in **HMHD**, where C_- has inverse and C_+ has both cascades [8].
- To determine direction of cascading we investigate **absolute equilibrium states** [1].
- The turbulence would relax into these states if not for the continual input of energy.
- We also prove that XMHD satisfies **Liouville theorem** in Fourier k space [1].
- To establish a bridge between MHD [9] and XMHD results we introduce Casimirs:

$$\text{magnetic- } H_M := \frac{1}{2} \frac{\kappa_+ C_- - \kappa_- C_+}{\kappa_+ - \kappa_-} = \frac{1}{2} \int d^3x (\mathbf{A}^* \cdot \mathbf{B}^* + d_e^2 \mathbf{V} \cdot \nabla \times \mathbf{V}), \quad (13)$$

$$\text{cross-helicity } H_C := \frac{1}{2} \frac{C_+ - C_-}{\kappa_+ - \kappa_-} = \int d^3x (\mathbf{V} \cdot \mathbf{B}^* + \frac{d_i}{2} \mathbf{V} \cdot \nabla \times \mathbf{V}), \quad (14)$$

$$\text{Phase space probability density } \mathcal{P} = Z^{-1} \exp[-\alpha H - \beta H_M - \gamma H_C] \quad (15)$$

The resulting states are plotted, for **HMHD** set $d_e = 0$, **IMHD** - $d_i = 0$;

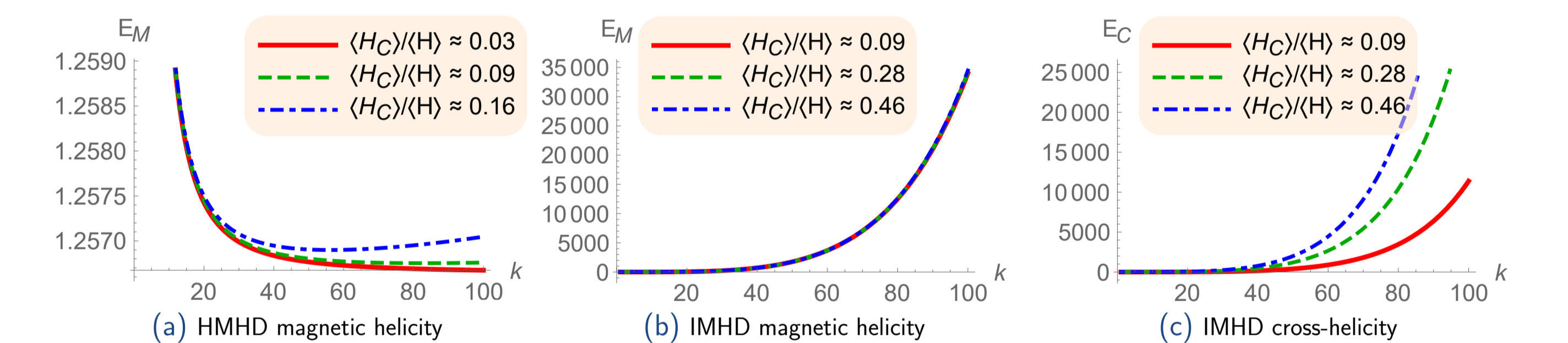


Figure: Absolute equilibria states of spectral quantities with parameters $\alpha = 10, \beta = 5$. (a) The HMHD regime, $d_e = 0.1$. The solid red line corresponds to $\langle H_C \rangle / \langle H \rangle \approx 0.03$, the dashed green line corresponds to $\langle H_C \rangle / \langle H \rangle \approx 0.09$, and the dot-dashed blue line corresponds to $\langle H_C \rangle / \langle H \rangle \approx 0.16$. The spectral range is chosen to be $1 < k < d_e^{-2}$. (b) IMHD magnetic helicity, $d_e = 0.1$. (c) IMHD cross-helicity with $\langle H_C \rangle / \langle H \rangle \approx 0.09$, $\langle H_C \rangle / \langle H \rangle \approx 0.28$, $\langle H_C \rangle / \langle H \rangle \approx 0.46$, $1 < k < d_e^{-2}$.

- Inverse cascade** is predicted only for magnetic helicity in **HMHD** range if $H_C \ll H$.
- IMHD** range is characterized by **direct cascades** for energy, and both helicities.

Short Summary

We have used the noncanonical Hamiltonian formulation of extended MHD models to arrive at their common mathematical structure, which manifests itself via the existence of generalized helicities and Lie-dragged 2-forms. These helicities, which are topological invariants, can be further studied through a host of techniques, including the Jones polynomial. We expect that in 3D turbulence the (generalized) magnetic helicity undergoes inverse cascade up to a certain length scale (for a given choice of the free parameters), and then undergoes a **cascade reversal**. When electron inertia effects were taken to be dominant over the Hall term (IMHD regime) we found that equipartition that was lost in HMHD was recovered.

References

G. Miloshevich, M. Lingam, P. J. Morrison Submitted to New J. Phys. (2016)
 G. Miloshevich, M. Lingam, P. J. Morrison https://arxiv.org/pdf/1610.04952.pdf (2016)
 M. Lingam, G. Miloshevich and P. J. Morrison Phys. Lett. A 380, 2400 (2016)
 H.M. Abdelhamid, Y. Kawazura, and Z. Yoshida J. Phys. A Math. Gen. 48, 235502 (2015)
 M. Lingam, P. J. Morrison and G. Miloshevich Phys. Plasmas 22, 072111 (2015)
 S. Benerjee and S. Galtier Phys. Rev. E, 93, 033120 (2016)
 R.H. Kraichnan and D. Montgomery Rev. Mod. Phys. 43, 547, 1971
 X. Liu and R.L. Ricca J. Phys. A 45, 205501 (2012)
 U. Frisch, A. Pouquet, J. Loraux, and A. Mazure J. Fluid Mech. 68, 769 (1975)